



HAL
open science

Lipase diffusion in oil-filled, alginate micro- and macrobeads

Pauline van Leusden, Gertjan J. M. den Hartog, Aalt Bast, Michiel Postema,
Erik van Der Linden, Leonard M.C. Sagis

► **To cite this version:**

Pauline van Leusden, Gertjan J. M. den Hartog, Aalt Bast, Michiel Postema, Erik van Der Linden, et al.. Lipase diffusion in oil-filled, alginate micro- and macrobeads. Food Hydrocolloids, 2018, 85, pp.242-247. 10.1016/j.foodhyd.2018.07.028 . hal-03192786

HAL Id: hal-03192786

<https://hal.science/hal-03192786>

Submitted on 15 Apr 2021

HAL is a multi-disciplinary open access archive for the deposit and dissemination of scientific research documents, whether they are published or not. The documents may come from teaching and research institutions in France or abroad, or from public or private research centers.

L'archive ouverte pluridisciplinaire **HAL**, est destinée au dépôt et à la diffusion de documents scientifiques de niveau recherche, publiés ou non, émanant des établissements d'enseignement et de recherche français ou étrangers, des laboratoires publics ou privés.



Distributed under a Creative Commons Attribution - NonCommercial - NoDerivatives 4.0
International License

1 Lipase diffusion in oil-filled, alginate micro- and
2 macrobeads

3

4 Authors: P. van Leusden¹, G.J.M. den Hartog², A. Bast², M. Postema³, E. van der Linden¹,
5 L.M.C. Sagis^{1*}

6 *1 Physics and Physical Chemistry of Foods Group, Department of Agrotechnology and Food*
7 *Sciences, Wageningen University, Bornse Weilanden 9, 6708 WG Wageningen, The*
8 *Netherlands*

9 *2 Department of Pharmacology and Toxicology, Maastricht University, PO Box 616, 6200*
10 *MD Maastricht, The Netherlands*

11 *3 School of Electrical and Information Engineering, Chamber of Mines Building, University*
12 *of the Witwatersrand, 1 Jan Smuts Avenue, Braamfontein, Johannesburg 2050, South Africa.*

13

14 Keywords: Oil digestion, microbeads, encapsulation, diffusion, Maxwell-Cattaneo equation

15

16

17 * Corresponding author

18 Email address: leonard.sagis@wur.nl

19 Abstract

20 Triglycerides, which are broken down in the lower part of the intestinal tract, give a stronger
21 ileal brake feedback, resulting in a feeling of satiety and causing people to eat less. The
22 digestion of triglycerides into fatty acids by lipase in the intestine can be delayed by
23 encapsulating oil droplets. In this study the release of fatty acids and oil droplet breakdown in
24 a simulated intestinal system was investigated, for oil droplets encapsulated in alginate micro-
25 (10.7 μm) and macrobeads (1.77 mm). It was found that fatty acid release rate was greatly
26 decreased by encapsulating the oil droplets into an alginate matrix compared to loose droplets.
27 Microscopic imaging of the breakdown of the oil droplets showed a sharp front moving from
28 the bead interface to the centre of the bead, and the change in position of the front scaled
29 linear with time. The motion of the front is well described by combining the mass balance for
30 lipase with a Maxwell-Cattaneo type equation, for the mass flux vector. The front in
31 microbeads seemed to move slightly slower ($0.15 (\pm 0.04) \mu\text{m}$ per minute) than for the
32 macrobeads ($0.20 (\pm 0.02) \mu\text{m}$ per minute). The release of free fatty acids in microbeads was
33 faster than in macrobeads, despite the slower front movement, because of the larger amount of
34 surface area available.

35 1. Introduction

36 Lipids which are digested in the ileum of the intestinal tract induce a negative feedback
37 mechanism, which increases feelings of satiety, causing people to eat less (Alleleyn, van
38 Avesaat, Troost, & Masclee, 2016; Maljaars, et al., 2011; Spiller, et al., 1984; Welch,
39 Saunders, & Read, 1985). This effect is called the ileal brake, and is stronger the further along
40 in the intestinal tract the lipids are digested (Welch, et al., 1985). Forcing lipids to be digested
41 further down the intestinal tract might have an application in the treatment or prevention of
42 obesity. Lipase is an enzyme, which breaks down triglycerides into glycerol and free fatty
43 acids (FFA), and is active at the oil-water interface. Therefore most systems intending to
44 delay lipid digestion are based on decreasing the accessibility of lipase to the triglyceride
45 interface. One method to slow the diffusion of lipase to the oil-water interface is by
46 encapsulating oil droplets into a hydrogel bead, where the porous gel acts as a barrier between
47 the lipase and the oil droplets (Corstens, et al., 2017; Li, Hu, Du, Xiao, & McClements, 2011).
48 Because the lipase first has to diffuse through the matrix before it reaches the oil droplet
49 interface, fatty acid release can be slowed down until the ileum is reached.

50 Alginate is a polysaccharide that has often been used for medical purposes, including
51 encapsulation of cells and drugs (Covarrubias, de-Bashan, Moreno, & Bashan, 2012; Lee &
52 Heo, 2000; Lim & Sun, 1980; J. Liu, et al., 2010; Pasparakis & Bouropoulos, 2006; Sultana,
53 et al., 2000). It is a non-toxic and biodegradable polymer which gels in the presence of
54 divalent cations. The method of gelation is very gentle, and thus appropriate for compounds
55 sensitive to heat or strong chemicals. Paques et al. developed a water-in-oil emulsification
56 method that is capable of creating beads of approximately 10 μm (Paques, van der Linden,
57 Sagis, & van Rijn, 2012; van Leusden, et al., 2017). Because particles smaller than 25 μm do
58 not negatively affect sensorial aspects of food, these microbeads can be added without
59 affecting sensorial perception (Tyle, 1993).

60 The factors that influence the rate of diffusion of components in gels include: gel type (X. C.
61 Liu, et al., 2002; Martinsen, Storrø, & Skjærk-Bræk, 1992) and density (Corstens, et al., 2017;
62 Martinsen, et al., 1992)), the diffusing component's size (Stewart & Swaisgood, 1993), shape
63 (Pluen, Netti, Jain, & Berk, 1999), and charge (Huguet & Dellacherie, 1996; Stewart, et al.,
64 1993), and environmental conditions such as pH (Huguet, et al., 1996) and ionic strength
65 (Huguet, et al., 1996; Stewart, et al., 1993; van Leusden, et al., 2017). In diffusion in
66 hydrogel beads, also the size of the beads is important (Corstens, et al., 2017; Li, et al., 2011).

67 When oil is encapsulated in alginate beads for the delayed release of fatty acids, one cannot
68 change the component (lipase) or environment, because those are naturally present in the
69 human biological system. We can however, control the gel properties. Li et al. showed that
70 the digestion of oil droplets encapsulated in alginate beads decreased with increasing bead
71 size (0.8 to 3.4 mm), and increased degree of cross-linking with calcium (Li, et al., 2011).
72 Corstens et al. also showed that digestion of oil droplets encapsulated in alginate beads
73 decreased with increasing bead size (0.55 to 1.15 mm), and with increasing alginate
74 concentration, which influences the mesh size of the alginate gel (Corstens, et al., 2017).

75 Encapsulating oil droplets in an indigestible hydrogel matrix delays the release of fatty acids
76 in the intestinal tract. The rate of the digestion is entirely dependent on the rate with which
77 lipase is able to diffuse into the bead and reach the oil droplets. In this study we investigated
78 the diffusion of lipase in gelled alginate beads. We investigated the influence of size in a
79 wider range than previously reported: macrobeads of 1.77 mm vs. microbeads of 10.7 μm . We
80 determined the rate of free fatty acid release, for both macro and microbeads, and used
81 microscopic imaging to track the breakdown of oil droplets as a function of time. We then
82 model this process by combining the mass balance for diffusion of lipase in the bead with a
83 Maxwell-Cattaneo type equation for the mass flux vector.

84

85 2. Materials and methods

86 2.1 Materials

87 CaCl₂·2H₂O, ethanol absolute, NaOH, NaCl (Merck millipore, Darmstadt, Germany), Tween
88 60, Lipase from porcine pancreas (Sigma, Steinheim, Germany), Polyglycerol polyricinoleate
89 (PGPR) 90 Kosher (Danisco, Copenhagen, Denmark), Medium Chain Triglycerides (MCT)
90 (Miglyol 812 N, Sasol, Germany), and Sodium alginate extracted from brown algae (Algin,
91 Texturas, Barcelona, Spain), were all used as received. Solutions were made in demineralized
92 water.

93 2.2 Production of Calcium crystals

94 Calcium crystals were made according to the method of Paques et al. (Paques, van der
95 Linden, van Rijn, & Sagis, 2012). In short: A dispersion was made of 6% PGPR in MCT oil
96 and allowed to mix for 2 hours. A volume of 5% of a 0.1 molal CaCl₂·2H₂O solution in
97 ethanol was added to this MCT solution and emulsified (Sonicator S-250A sonicator, Branson
98 Ultrasonics, USA) for 2 minutes. The resulting mixture was heated and stirred overnight at 60
99 °C without cover to allow the ethanol to evaporate, producing a dispersion of calcium crystals
100 in oil.

101 2.3 Production of the microbeads

102 Oil filled alginate microbeads were made based on the method described by Van Leusden et
103 al. (van Leusden, et al., 2017). The inner oil droplets were made by mixing 5.0% (w/w) MCT
104 with demi-water containing 0.3% (w/w) Tween 60 with an Ultra-Turrax (Ultra-Turrax T 25,
105 IKA Werke, Germany) at 8000 rpm for 2 minutes. The emulsion was further homogenized
106 (Delta instruments, Drachten, The Netherlands) at 180 bar for 3 passes. To the emulsion 2.0%
107 (w/w) alginate was added and allowed to dissolve for 2 hours. While mixing with the Ultra-
108 Turrax at 8800 rpm, 10% (v/v) of the previous emulsion was slowly added to MCT oil
109 containing 4% (w/w) PGPR. After full addition the double emulsion was mixed for a further 3
110 minutes. After mixing, 5 mL of calcium crystal dispersion was added per mL of primary
111 emulsion. This mixture was gently stirred for at least 18 hours to allow gelation of the beads.

112 The beads were removed from the oil phase by successive centrifugation and redispersion
113 steps. The beads were centrifuged for 2 hours at 3500 g. The pellet was redispersed in 25 mM
114 CaCl₂ solution, homogenised at 100 bar for 3 passes and then once again centrifuged at 1000

115 g for 1 hour. The sediment was redispersed in demi-water, after which the centrifugation was
116 repeated. The highly concentrated beads were stored in demi-water and diluted before use.

117 2.4 Production of the macrobeads

118 Oil filled alginate macrobeads were made based on the method described by (van Leusden, et
119 al., 2017). The inner oil droplets with alginate were made as described in the section of the
120 production of microbeads. The emulsion was put in a syringe and expressed through a needle
121 of 0.3 mm (BD Microlance 0.3x13 mm) into a 25 mM CaCl₂ water bath, where the droplets
122 were formed approximately 5 cm above water level. The beads were stirred for 1 hour and
123 then stored in the CaCl₂ solution, at 4 °C, for a further 24 hours. The beads were taken from
124 the CaCl₂ solution, the excess CaCl₂ solution was absorbed with filter paper, and the beads
125 were stored at high concentrations in demi-water.

126 2.5 Size determination

127 The size of the beads was measured by light microscopy (Axioskop 50) equipped with a
128 camera (AxioCam HRc) (both from Zeiss, Germany). Images were analysed with ImageJ.

129 2.6 Lipase accessibility

130 The lipase accessibility to the oil droplets was investigated in: 1) a 2.0% (v/v) dispersion of
131 microbeads, 2) a 2.0% (v/v) dispersion of macrobeads, 3) an equivalent amount of non-
132 encapsulated emulsion, as made for the production of the alginate beads, but before addition
133 of the alginate. The volume fraction was estimated by drying samples of the beads overnight
134 in an oven at 105°C. The dry weight of the beads was used to calculate the volume fraction of
135 the beads, assuming no loss of oil occurred. The accessibility was measured in a diluted,
136 simulated intestinal system based on the system described by (Minekus, et al., 2014). This
137 consisted of 150 mM of NaCl and 1 mg/mL pancreatic lipase at pH 7.0 and 37 °C. The
138 conversion of MCT to the acidic fatty acids was followed by the amount of NaOH that needed
139 to be added to keep the pH at 7.0. This was done with the pH-STAT (Metrohm, Herisau,
140 Switzerland). The reaction was followed for 2.5 hours and duplicate experiments were
141 performed. The free fatty acid release was calculated with the following equation:

$$142 \text{ FFA \%} = \frac{V_{\text{NaOH}} M_{\text{NaOH}} M_{\text{w,lipid}}}{3\omega_{\text{lipid}}}$$

143 where V_{NaOH} is the volume of NaOH titrated into the solution to keep it at pH 7.0, M_{NaOH} the
144 molarity of the NaOH solution, $M_{\text{w,lipid}}$ the average molecular weight of the MCT oil, which

145 was calculated to be 508 g/mol (based on the composition specified by the manufacturer), and
146 ω_{lipid} the fraction of lipid present in the beginning of the experiment. The factor 3 is present
147 because every triglyceride contains 3 fatty acids which can be released.

148 The oil droplet breakdown was also followed with light microscopy. The same method as for
149 the pH-STAT was used, and at regular time intervals a small sample of the solution was
150 taken. The sample was immediately heated to 80°C for 10 minutes to inactivate the lipase. For
151 every sample at least 25 microbeads were investigated in the range of 9.0 to 12 μm . The
152 macrobeads were cut in half and viewed in a microscope slide with a dip, to prevent the
153 pressure of the cover slide to influence the measurements. For every sample at least four
154 macrobeads were investigated, and the location of the breakdown front was determined at
155 different points along the circumference of the bead.

156 3. Results and Discussion

157 3.1 FFA digestion and release

158 The amount of free fatty acids (FFA) released from oil droplets encapsulated in microbeads
159 and macrobeads, and non-encapsulated droplets, over time is presented in Figure 1.

160 Approximately 70% of the lipids of the non-encapsulated droplets were digested and released
161 from the oil droplets within 6 minutes. After this point, the breakdown proceeds more slowly.
162 This change in rate could be the result of the fact that pancreatic lipase can cut the fatty acids
163 from the 1 and 3 position from the glycerol backbone very quickly, while the fatty acid from
164 the 2 position of the monoglyceride occurs only after isomerisation of the monoglyceride
165 (Borgström, 1964; Korn, 1961; Mattson & Beck, 1956). In addition, as a result of the
166 breakdown, the available surface area is reduced, and the fraction of lipase which participates
167 in the process is reduced.

168 As can be seen in Figure 1, the rate of lipolysis of encapsulated oil droplets is far slower than
169 for non-encapsulated droplets. Lipase first needs to diffuse to the oil-water interface of the oil
170 droplets, and adsorb at this interface. For non-encapsulated droplets in a stirred vessel, this
171 adsorption process is fast. For encapsulated oil droplets, lipase first has to diffuse through the
172 gel matrix of the beads before it can adsorb at the oil-water interface (Corstens, et al., 2017;
173 Li, et al., 2011). After 2.5 hours, 9.0% of the lipids in the macrobeads has been broken down.
174 The amount of FFA released is almost linear in time, which means the release rate is nearly
175 constant up to 150 min. For the microbeads, after 150 min, approximately 80% of the lipids
176 has been broken down. Here, the rate of lipid breakdown decreases over time. The difference
177 between micro- and macrobeads can be explained by the difference in specific surface area of
178 the beads. It is known that lipase diffuses more slowly through a gelled matrix than in a
179 solution.

180 The progression of oil droplet breakdown in time in macro- and microbeads was followed by
181 microscopy (Figure 2, and 3).

182 As can be seen from the images, for both the micro- and macrobeads there appears to be a
183 front moving inwards over time, separating a volume where oil-droplets have been broken
184 down, from a volume where they appear to be unaffected. The fact that an inward moving
185 front is visible indicates that the breakdown process is diffusion limited, and that the diffusion
186 process itself is non-Fickian. From a previous study it is known that BSA, which has a radius

187 of 3.9 nm (Pluen, et al., 1999), diffuses throughout similarly made micro- and macrobeads
188 within several minutes (van Leusden, et al., 2017). Lipase is smaller than BSA (2.8 nm)
189 (Pignol, et al., 2000) and the salt concentration in the current study is higher (100 vs. 150 mM
190 NaCl), so we would expect lipase diffusion through the gel matrix of the bead to be faster.
191 However, when the lipase diffuses into the beads and encounters an oil droplet, it will adsorb
192 on the oil-water interface, and will essentially be trapped there until the oil droplet is digested.
193 When the volume fraction of encapsulated droplets is high enough, this trapping will result in
194 an *effective* diffusion process with a non-Fickian appearance. Additionally, it is possible that
195 the presence of the lipase in the pores of the alginate gel may thereby also block other lipase
196 molecules of diffusing through.

197 3.2 Displacement of the oil front

198 The displacements of the fronts for both macro and microbeads were determined from image
199 analysis of Figure 2, and Figure 3. The results are shown in Figure 4.

200 For the macrobeads, the displacement of the front is linear in time, which corresponds to the
201 release of FFA, which was also linear in time. After 2.5 hours, the front has moved
202 approximately 30 μm inwards. The amount of oil in this 30 μm shell corresponds to
203 approximately 9.7% of the total oil content. As shown in Figure 1, the release rate after 2.5
204 hours is approximately 9.0%. This confirms that the breakdown of oil indeed proceeds from
205 the outward in.

206 The displacement of the front in the microbeads is also linear in time. The oil of the beads
207 with a diameter in the range of 9 to 12 μm is mostly broken down within 80 minutes, which is
208 in reasonable agreement with the FFA release data. The difference between these two
209 measurements is the result of the polydispersity of the beads. For our image analysis we
210 investigated mainly beads between 9 and 12 μm . There is however also a fraction of beads
211 smaller than 9 μm and another fraction of beads larger than 12 μm . Larger beads release their
212 oil slowly, because of their lower specific surface area. After 2.5 hours there were still several
213 bigger microbeads, of approximately 50 μm , that still had not released all their oil, and this is
214 why in the FFA release graph only 80% of the oil of the microbeads is released. The rate of
215 front displacement in the macrobeads is approximately 0.20 (± 0.02) μm per minute, while for
216 the microbeads this is approximately 0.15 (± 0.04) μm per minute (calculated from the average
217 bead size of 10.7 μm).

218 3.3 Modelling of lipolysis kinetics

219 Both Li et al. and Corstens et al. have developed models for the diffusion of lipase through
220 alginate microbeads (Corstens, et al., 2017; Li, et al., 2011). The model of Li et al. did not fit
221 the experimental results very well, for which they give several possible explanations. The
222 pore size they assumed is most likely much smaller than the actual pore size, as found by
223 Corstens et al., which dramatically reduces the diffusion coefficient. They also suggest that
224 lipase may interact with the gel network, where we assume that lipase in fact interacts with
225 the oil droplets, thereby also resulting in hindered diffusion.

226 Corstens et al. have used Fick's law to calculate the concentration of enzyme at a certain
227 position in their beads. For the large beads we will assume the effects of curvature are
228 negligible, and we will describe the diffusion process as a one-dimensional diffusion problem
229 in a Cartesian coordinate system (x,y,z) . According to Fick's law the mass flux of lipase in the
230 x -direction is given by

$$231 \quad J_x = -D \frac{\partial C}{\partial x} \quad (1)$$

232 Where J_x is the flux in $\text{mol/m}^2\text{s}$, D is the diffusion coefficient in m^2/s , and c is the
233 concentration in mol/m^3 .

234 A drawback of this model is that when combined with the mass balance for lipase, we obtain
235 a parabolic partial differential equation, which predicts an unbounded speed of propagation of
236 concentration perturbations. In our case however we have seen a clear front moving through
237 the bead at a finite speed. To alleviate this problem we replace Eq. (1) by a Maxwell-Cattaneo
238 type equation for the mass flux. The Maxwell-Cattaneo equation is an adaption of Fourier's
239 law for heat conduction, where a characteristic time is introduced to avoid an unbounded
240 speed of propagation of thermal perturbations (Jou, Casas-Vázquez, & Lebon, 2010). For
241 mass diffusion this equation is formulated as:

$$242 \quad \tau \frac{\partial J_x}{\partial t} + J_x = -D \frac{\partial C}{\partial x} \quad (2)$$

243 Here t is time, and τ is the retardation time, in s. Combining this expression for the mass flux
244 with the differential mass balance for lipase, we obtain (see Appendix)

$$245 \quad \frac{\partial^2 C}{\partial t^2} + \frac{1}{\tau} \frac{\partial C}{\partial t} - \frac{D}{\tau} \frac{\partial^2 C}{\partial x^2} = 0 \quad (3)$$

246 This is a telegraph equation, a hyperbolic partial differential equation which predicts a finite
247 speed of propagation for concentration perturbations, v , given by:

$$248 \quad v = \sqrt{\frac{D}{\tau}} \quad (4)$$

249 When v is constant, (3) predicts a front displacement L for the large beads, which is linear in
250 time, i.e.

$$251 \quad L \sim \left(\sqrt{\frac{D}{\tau}} \right) t \quad (5)$$

252 For the small beads, following along the same lines, we also find a relative front displacement
253 which is linear in time. Both scalings are confirmed by our experimental results (see Fig. 4).

254 To establish the limits of validity of the model we present here, and compare it to the other
255 models (Corstens, et al., 2017; Li, et al., 2011), we need to consider the processes of
256 diffusion, adsorption and digestion in more detail. The beads are a complex multiphase
257 system, in which the lipase diffuses through the matrix of the bead (and interacts with this
258 matrix), until it encounters an oil droplet. It then adsorbs at the interface, after which it starts
259 to digest the oil droplet. After digestion, the desorbed lipase can continue its path through the
260 matrix, until it reaches another droplet. By assuming Eq (2) we describe this complex
261 diffusion-adsorption-reaction system on a coarse-grained level, and approximate the structure
262 of the beads as a single effective medium. On this coarse-grained level the diffusion of the
263 lipase through the bead is quantified by the coefficient D . On its path the lipase is retarded by
264 the matrix and by adsorption to the oil droplets, and this is characterized by the retardation
265 time. Such a coarse-grained model will give good results, as long as the matrix is
266 homogeneous, with small pores, and oil droplets are small and homogeneously dispersed
267 throughout the bead.

268 In systems with small pores and homogeneously dispersed droplets the retardation time will
269 be longer, which will give a slower propagation speed. In systems with bigger pores and
270 small numbers of large oil droplets the retardation time will be shorter, thereby increasing the
271 propagation speed. For such systems the process will more closely resemble the diffusion
272 according to Fick's second law (note that Eq (2) reduces to that equation in the limit that τ
273 goes to zero). Corstens et al. have used Fick's law to describe their systems (Corstens, et al.,
274 2017). This gave a good description of their data since their beads contained a small number

275 of large oil droplets ($D_{32} = 21 \pm 4 \mu\text{m}$), whereas ours contain a large number of relatively
276 small ones (approximately $1 \mu\text{m}$). The surface to volume ratio is smaller in larger droplets,
277 and therefore less surface is available for lipase entrapment. In their study the retardation
278 effects are therefore much smaller. The model of Corstens et al. has proven to be adequate for
279 several alginate macrobead systems. In our system however, where a clear, linear front was
280 visible over a prolonged length of time, retardation effects were significant, and the Maxwell-
281 Cattaneo equation provided a better description of the dynamics of the system.

282

283 4. Conclusions

284 Lipid digestion was slowed by encapsulating oil droplets into an alginate matrix, because the
285 alginate creates a barrier that lipase first has to diffuse through before it is able to attach to the
286 interface of the oil droplets. Once lipase is bound at the interface it is trapped until the droplet
287 is digested, which retards lipase diffusion. The breakdown of oil droplets in the alginate beads
288 proceeded from the outside of the bead to the centre, where a clear front was present during
289 digestion. The progression of the front was linear and could be described best by a Maxwell-
290 Cattaneo type equation for the mass flux, instead of the normally used Fick's law. For
291 microbeads this front seemed to move slightly slower at $0.15 (\pm 0.04) \mu\text{m}$ per minute than for
292 macrobeads, $0.20 (\pm 0.02) \mu\text{m}$ per minute. Despite the similar front speed, the oil in the
293 microbeads digested much faster than the oil in macrobeads because of the larger amount of
294 surface area available.

295

296 5. Acknowledgements

297 The research presented in this paper was financially supported by the Graduate School
298 VLAG, of Wageningen University.

299

300 References

301

- 302 Alleleyn, A., van Avesaat, M., Troost, F., & Masclee, A. (2016). Gastrointestinal Nutrient
303 Infusion Site and Eating Behavior: Evidence for A Proximal to Distal Gradient within
304 the Small Intestine? *Nutrients*, 8(3), 117.
- 305 Borgström, B. (1964). Influence of bile salt, pH, and time on the action of pancreatic lipase;
306 physiological implications. *Journal of lipid research*, 5(4), 522-531.
- 307 Corstens, M. N., Berton-Carabin, C. C., Elichiry-Ortiz, P. T., Hol, K., Troost, F. J., Masclee,
308 A. A. M., & Schroën, K. (2017). Emulsion-alginate beads designed to control in vitro
309 intestinal lipolysis: Towards appetite control. *Journal of Functional Foods*,
310 34(Supplement C), 319-328.
- 311 Covarrubias, S. A., de-Bashan, L. E., Moreno, M., & Bashan, Y. (2012). Alginate beads
312 provide a beneficial physical barrier against native microorganisms in wastewater
313 treated with immobilized bacteria and microalgae. *Applied Microbiology and*
314 *Biotechnology*, 93(6), 2669-2680.
- 315 Huguet, M. L., & Dellacherie, E. (1996). Calcium alginate beads coated with chitosan: Effect
316 of the structure of encapsulated materials on their release. *Process Biochemistry*,
317 31(8), 745-751.
- 318 Jou, D., Casas-Vázquez, J., & Lebon, G. (2010). Extended Irreversible Thermodynamics:
319 Evolution Equations. In *Extended Irreversible Thermodynamics* (pp. 42-58).
320 Dordrecht: Springer Netherlands.
- 321 Korn, E. D. (1961). The fatty acid and positional specificities of lipoprotein lipase. *Journal of*
322 *Biological Chemistry*, 236(6), 1638-1642.
- 323 Lee, K.-Y., & Heo, T.-R. (2000). Survival of Bifidobacterium longum Immobilized in calcium
324 alginate beads in simulated gastric juices and bile salt solution. *Applied and*
325 *Environmental Microbiology*, 66(2), 869-873.
- 326 Li, Y., Hu, M., Du, Y., Xiao, H., & McClements, D. J. (2011). Control of lipase digestibility
327 of emulsified lipids by encapsulation within calcium alginate beads. *Food*
328 *Hydrocolloids*, 25(1), 122-130.
- 329 Lim, F., & Sun, A. M. (1980). Microencapsulated islets as bioartificial endocrine pancreas.
330 *Science*, 210(4472), 908-910.
- 331 Liu, J., Zhang, Y., Wang, C., Xu, R., Chen, Z., & Gu, N. (2010). Magnetically sensitive
332 alginate-templated polyelectrolyte multilayer microcapsules for controlled release of
333 doxorubicin. *The Journal of Physical Chemistry C*, 114(17), 7673-7679.
- 334 Liu, X. C., Yu, W. Y., Zhang, Y., Xue, W. M., Yu, W. T., Xiong, Y., Ma, X. Y., Chen, Y., &
335 Yuan, Q. (2002). Characterization of structure and diffusion behaviour of Ca-alginate
336 beads prepared with external or internal calcium sources. *Journal of*
337 *Microencapsulation*, 19(6), 775-782.
- 338 Maljaars, P., Peters, H. P., Kodde, A., Geraedts, M., Troost, F. J., Haddeman, E., & Masclee,
339 A. A. (2011). Length and site of the small intestine exposed to fat influences hunger
340 and food intake. *British journal of nutrition*, 106(10), 1609-1615.
- 341 Martinsen, A., Storrø, I., & Skjærk-Bræk, G. (1992). Alginate as immobilization material: III.
342 Diffusional properties. *Biotechnology and Bioengineering*, 39(2), 186-194.
- 343 Mattson, F., & Beck, L. (1956). The specificity of pancreatic lipase for the primary hydroxyl
344 groups of glycerides. *Journal of Biological Chemistry*, 219(2), 735-740.
- 345 Minekus, M., Alminger, M., Alvito, P., Ballance, S., Bohn, T., Bourlieu, C., Carrière, F.,
346 Boutrou, R., Corredig, M., & Dupont, D. (2014). A standardised static in vitro

347 digestion method suitable for food—an international consensus. *Food & function*, 5(6),
348 1113-1124.

349 Paques, J. P., van der Linden, E., Sagis, L. M. C., & van Rijn, C. J. M. (2012). Food-Grade
350 Submicrometer Particles from Salts Prepared Using Ethanol-in-Oil Mixtures. *Journal*
351 *of Agricultural and Food Chemistry*, 60(34), 8501-8509.

352 Paques, J. P., van der Linden, E., van Rijn, C. J. M., & Sagis, L. M. C. (2012). Alginate
353 submicron beads prepared through w/o emulsification and gelation with CaCl₂
354 nanoparticles. *Food Hydrocolloids*, 31(2), 428-434.

355 Pasparakis, G., & Bouropoulos, N. (2006). Swelling studies and in vitro release of verapamil
356 from calcium alginate and calcium alginate–chitosan beads. *International Journal of*
357 *Pharmaceutics*, 323(1–2), 34-42.

358 Pignol, D., Ayzavian, L., Kerfelec, B., Timmins, P., Crenon, I., Hermoso, J., Fontecilla-
359 Camps, J. C., & Chapus, C. (2000). Critical role of micelles in pancreatic lipase
360 activation revealed by small angle neutron scattering. *Journal of Biological Chemistry*,
361 275(6), 4220-4224.

362 Pluen, A., Netti, P. A., Jain, R. K., & Berk, D. A. (1999). Diffusion of Macromolecules in
363 Agarose Gels: Comparison of Linear and Globular Configurations. *Biophysical*
364 *journal*, 77(1), 542-552.

365 Spiller, R., Trotman, I., Higgins, B., Ghatei, M., Grimble, G., Lee, Y., Bloom, S., Misiewicz,
366 J., & Silk, D. (1984). The ileal brake--inhibition of jejunal motility after ileal fat
367 perfusion in man. *Gut*, 25(4), 365-374.

368 Stewart, W. W., & Swaisgood, H. E. (1993). Characterization of calcium alginate pore
369 diameter by size-exclusion chromatography using protein standards. *Enzyme and*
370 *microbial technology*, 15(11), 922-927.

371 Sultana, K., Godward, G., Reynolds, N., Arumugaswamy, R., Peiris, P., & Kailasapathy, K.
372 (2000). Encapsulation of probiotic bacteria with alginate-starch and evaluation of
373 survival in simulated gastrointestinal conditions and in yoghurt. *International Journal*
374 *of Food Microbiology*, 62(1-2), 47-55.

375 Tyle, P. (1993). Tactile Pattern Recognition Effect of size, shape and hardness of particles in
376 suspension on oral texture and palatability. *Acta Psychologica*, 84(1), 111-118.

377 van Leusden, P., den Hartog, G. J. M., Bast, A., Postema, M., van der Linden, E., & Sagis, L.
378 M. C. (2017). Permeation of probe molecules into alginate microbeads: Effect of salt
379 and processing. *Food Hydrocolloids*, 73(Supplement C), 255-261.

380 Welch, I., Saunders, K., & Read, N. W. (1985). Effect of ileal and intravenous infusions of fat
381 emulsions on feeding and satiety in human volunteers. *Gastroenterology*, 89(6), 1293-
382 1297.

383

384

385 Appendix

386 Derivation of equation (3)

387 We start by rewriting (2) as:

$$388 \quad \frac{\partial J_x}{\partial t} = -\frac{D}{\tau} \frac{\partial C}{\partial x} - \frac{1}{\tau} J_x \quad (\text{A.1})$$

389 In a Cartesian coordinate system the mass balance for the lipase is given by:

$$390 \quad \frac{\partial C}{\partial t} = -\frac{\partial J_x}{\partial x} \quad (\text{A.2})$$

391 Taking the derivative with respect to time of this equation, we obtain:

$$392 \quad \frac{\partial^2 C}{\partial t^2} = -\frac{\partial}{\partial x} \left(\frac{\partial J_x}{\partial t} \right) \quad (\text{A.3})$$

393 Here we have used the fact that x and t are independent variables, and exchanged the order of
394 derivation in the term on the right hand side. When combining equations A.1 and A.3 we find:

$$395 \quad \frac{\partial^2 C}{\partial t^2} = \frac{\partial}{\partial x} \left(\frac{D}{\tau} \frac{\partial C}{\partial x} + \frac{1}{\tau} J_x \right) \quad (\text{A.4})$$

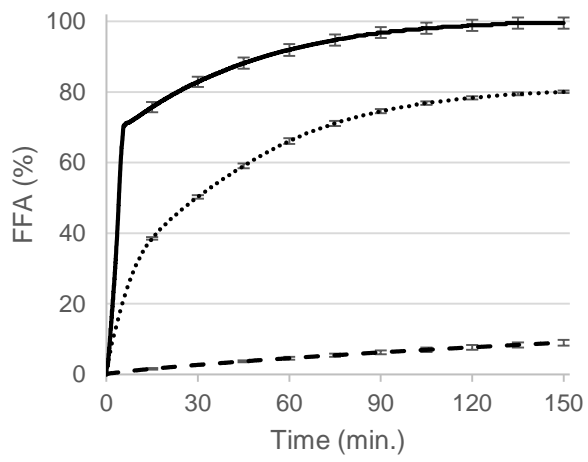
396 Eliminating the second term on the right hand side, using A.2, we obtain:

$$397 \quad \frac{\partial^2 C}{\partial t^2} + \frac{1}{\tau} \frac{\partial C}{\partial t} - \frac{D}{\tau} \frac{\partial^2 C}{\partial x^2} = 0 \quad (\text{A.5})$$

398

399 Figures:

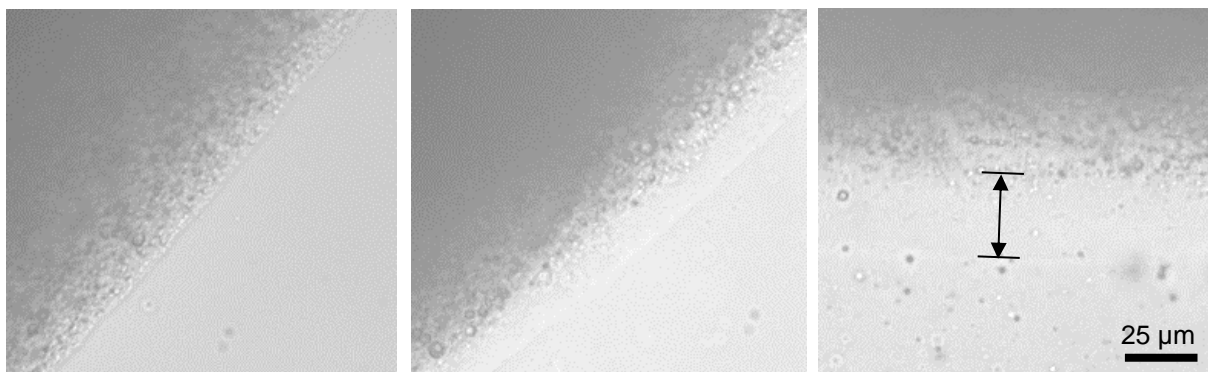
400 Figure 1:



401

402

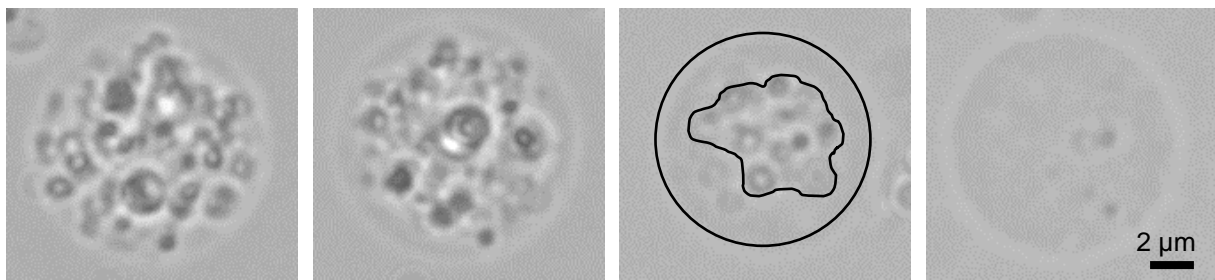
403 Figure 2:



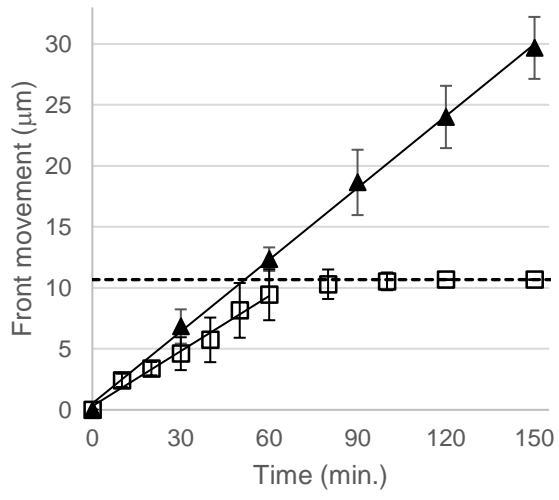
404

405

406 Figure 3:



409 Figure 4:



410